9266 *Biochemistry* **2009,** *48,* 9266–9277
DOI: 10.1021/bi901020d

BIOCHEMISTRY
including biophysical chemistry & molecular biology
Article

Engineered Socket Study of Signaling through a Four-Helix Bundle: Evidence for a Yin−Yang Mechanism in the Kinase Control Module of the Aspartate Receptor

Kalin E. Swain, Miguel A. Gonzalez, and Joseph J. Falke*

Department of Chemistry and Biochemistry and Molecular Biophysics Program, University of Colorado, Boulder, Colorado 80309-0215

Received June 17, 2009; Revised Manuscript Received August 22, 2009

ABSTRACT: The chemoreceptors of *Escherichia coli* and *Salmonella typhimurium* form stable oligomers that associate with the coupling protein CheW and the histidine kinase CheA to form an ultrasensitive, ultrastable signaling lattice. Attractant binding to the periplasmic domain of a given receptor dimer triggers a transmembrane conformational change transmitted through the receptor to its cytoplasmic kinase control module, a long four-helix bundle that binds and regulates CheA kinase. The kinase control module comprises three functional regions: the adaptation region possessing the receptor adaptation sites, a coupling region that transmits signals between other regions, and the protein interaction region possessing contact sites for receptor oligomerization and for CheA−CheW binding. On the basis of the spatial clustering of known signal locking Cys substitutions and engineered disulfide bonds, this study develops the yin−yang hypothesis for signal transmission through the kinase control module. This hypothesis proposes that signals are transmitted through the four-helix bundle via changes in helix−helix packing and that the helix packing changes in the adaptation and protein interaction regions are tightly and antisymmetrically coupled. Specifically, strong helix packing in the adaptation region stabilizes the receptor on state, while strong helix packing in the protein interaction region stabilizes the off state. To test the yin−yang hypothesis, conserved sockets likely to strengthen specific helix−helix contacts via knob-in-hole packing interactions were identified in the adaptation, coupling, and protein interaction regions. For 32 sockets, the knob side chain was truncated to Ala to weaken the knob-in-hole packing and thereby destabilize the local helix−helix interaction provided by that socket. We term this approach a "knob truncation scan". Of the 32 knob truncations, 28 yielded stable receptors. Functional analysis of the signaling state of these receptors revealed seven lock-off knob truncations, all located in the adaptation region, that trap the receptor in its "off" signaling state (low kinase activity, high methylation activity). Also revealed were five lock-on knob truncations, all located in the protein interaction region, that trap the "on" state (high kinase activity, low methylation activity). These findings provide strong evidence that a yin−yang coupling mechanism generates concerted, antisymmetric helix−helix packing changes within the adaptation and protein interaction regions during receptor on−off switching. Conserved sockets that stabilize local helix−helix interactions play a central role in this mechanism: in the on state, sockets are formed in the adaptation region and disrupted in the protein interaction region, while the opposite is true in the off state.

The homodimeric chemoreceptors of bacterial chemotaxis span the inner cell membrane. These receptors bind attractants in the periplasmic space and generate a transmembrane conformational change that regulates the activities of the cytoplasmic CheA kinase, ultimately controlling the swimming behavior of the bacterial cell and driving cellular chemotaxis up an attractant concentration gradient (reviewed in refs (*1*−*6*)). The oligomeric structure of the chemoreceptors is complex: each receptor homodimer associates with two other dimers to form a receptor trimer of dimers (*1*, *7*, *8*) (Figure 1). In turn, these trimers of dimers associate to form a hexagonal, two-dimensional array of trimers (*9*−*11*). All of the cytoplasmic components of the chemotaxis pathway assemble onto the receptor array, thereby generating a multiprotein signaling complex (*3*, *12*, *13*). The positive cooperativity between receptors provided by array organization is believed to be crucial to the ultrasensitivity of the pathway, which can detect exquisitely small changes in attractant concentration (*14*, *15*). The array organization is also likely to be essential for the recently discovered ultrastability of the isolated signaling complex, which exhibits a structural and functional half-life exceeding several days (*16*).

The chemoreceptor homodimer exhibits a modular structure built from collections of four-helix bundles (*1*, *8*, *17*, *18*) (Figure 1). The periplasmic ligand binding domain is a dimer of two antiparallel four-helix bundles. Two helices from each subunit associate to form a membrane-spanning, antiparallel four-helix bundle, in which the transmembrane signal is generated by the piston-type displacement of the signaling helix (*1*, *6*, *19*). In the cytoplasm, the signaling helix is coupled to the conserved HAMP domain, a parallel four-helix bundle that transduces the transmembrane piston signal into a different type of conformational change (*1*, *20*, *21*). This unidentified HAMP conformational change in turn regulates the on−off switching of the long, extended four-helix bundle termed the kinase control module (*1*).

*To whom correspondence should be addressed: Email falke@colorado.edu, Tel (303) 492-3503, Fax (303) 492-5894.

 Published on Web 08/25/2009

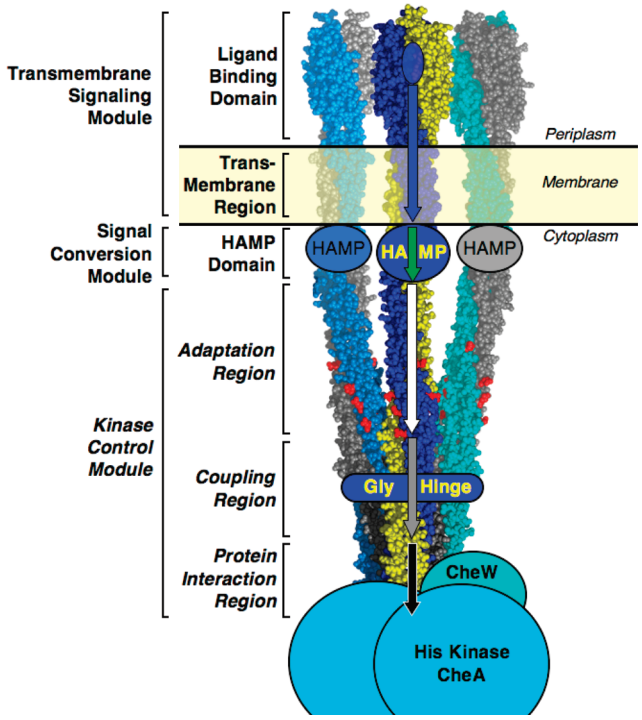

FIGURE 1: Schematic core complex illustrating different functional regions of the receptor. Shown is a receptor trimer of dimers (individual subunits are unique colors) in complex with the dimeric histidine kinase CheA (blue) and the coupling protein CheW (cyan). This core complex is believed to represent the minimal structural unit required for receptor-regulated kinase activity (*1*, *51*). The structural−functional regions investigated in this study are italicized. Attractant binding to the periplasmic ligand binding site is believed to trigger different types of conformational changes in each region denoted by a different arrow color, ultimately transmitting a regulatory signal to the bound CheA kinase. In the transmembrane signaling module, the conformational signal is a piston displacement of the signaling helix (blue arrow). The signal conversion or HAMP module converts this piston displacement into a different conformational signal (green arrow). The kinase control module is an extended four-helix bundle that carries information from HAMP to bound CheA and possesses three functional regions. The yin−yang hypothesis developed herein proposes that signal transmission through the regions of the four-helix bundle involves changes in helix−helix packing and that the polarities of these packing changes are opposite in the adaptation and protein interaction regions. The coupling region is essential for communication (gray arrow) of these helix packing changes between the two regions. While attractant binding and conformational changes are indicated in only one receptor dimer, positive cooperativity between receptors may generate corresponding conformational changes in the other dimers.

This study focuses on the conformational transitions that underlie on−off switching within the kinase control module and its three distinct functional regions: the adaptation region, the coupling region, also termed the flexible region (*22*), and the protein interaction region (*1*). The adaptation region possesses the conserved Glu residues that are methyl esterified and demethylated by the adaptation enzymes CheR and CheB, respectively, as well as a high density of other anionic residues that generate electrostatic repulsion between and within the helices of the four-helix bundle (*23*). The coupling region is less conserved than the other regions (*22*) except for a conserved Gly hinge that has been shown to enable the bundle to bend (*24*−*26*). The protein interaction region possesses the highly conserved interaction sites essential for trimer-of-dimer formation, and for binding the coupling protein CheW and the histidine kinase CheA in the ultrasensitive, ultrastable, signaling complex (*1*, *25*, *27*−*31*). During signal transduction, conformational signals arising from both attractant binding and covalent modification of the adaptation sites are transmitted through the adaptation, coupling, and protein interaction regions to the bound CheA kinase. The resulting kinase on−off switching controls both the motor regulation and adaptation branches of the pathway, which are each essential for chemotaxis.

Previous Cys and disulfide scanning studies of the adaptation and protein interaction regions have revealed a striking spatial pattern of effects on receptor function (*32*−*37*). In the adaptation region, one finds the highest density of lock-on disulfide bonds that covalently stabilize helix−helix packing between the two subunits of the homodimer and trap the receptor in its kinase-activating state (*33*, *36*). By contrast, in the protein interaction region, one finds the highest density of lock-on Cys substitutions that, in their reduced state, trap the receptor in its kinase-activating state, perhaps by weakening helix−helix interactions (*35*, *37*). Here we first confirm these earlier conclusions using the recently developed, antisymmetric activity method that enables positive identification of lock-on and lock-off modifications in the full-length, membrane-bound receptor (*19*). On the basis of the observed clustering of lock-on and lock-off modifications in different regions, we propose the yin−yang model for signal transmission between the adaptation and protein interaction regions. The model hypothesizes that the receptor "on" state possesses stable helix−helix packing in the adaptation region, which destabilizes helix−helix packing in the protein interaction region and activates CheA kinase. The reverse configuration is proposed to generate the receptor "off" state that inhibits CheA kinase.

To test the yin−yang hypothesis, a new "knob truncation scan" approach is developed to systematically perturb helix−helix interactions at specific locations by weakening local socket motifs, each of which consists of a knob side chain that inserts into a hole formed by four residues on an adjacent helix (*38*, *39*). The approach is applied to conserved sockets in the adaptation, coupling, and protein interaction regions of the full-length, membrane-bound receptor. The observed functional effects of the knob truncations strongly support the yin−yang hypothesis in which the helix−helix packing states of the adaptation and protein interaction regions are tightly coupled to each other but exhibit opposite signaling polarities.

MATERIALS AND METHODS

Materials. Reagents were obtained from the following sources: [γ-^{32}P]ATP from Perkin-Elmer, QuickChange site-directed mutagenesis kit from Stratagene, mutagenic oligonucleotides from Integrated DNA Technologies, and all other analytical grade chemicals from Sigma unless noted otherwise. *Escherichia coli* strains were graciously provided by J. S. Parkinson (University of Utah, Salt Lake City, UT).

Identification of Conserved Sockets Likely To Contribute to Helix−Helix Packing Stability. To select conserved sockets likely to stabilize helix−helix packing in the kinase control module, the program SOCKET by Woolfson and coworkers (*39*) was used to predict stable knob-in-holes packing interactions both in (i) the well-defined coupling and protein interaction regions of the published crystal structure (*8*, *17*) [Protein Data Bank (PDB) entry 1QU7, residues 323−462 and 323′−462′ of Tsr corresponding to residues 321−460 and

321′−460′ of Tar, respectively] and (ii) the modeled structure of the adaptation region based on chemical constraints (*8*, *17*, *33*, *34*) (residues 262−322, 262′−322′, 463−522, and 463′−522′ of Tsr corresponding to residues 260−320, 260′−320′, 461−520, and 461′−520′ of Tar, respectively). A cutoff value of 7.8 Å was used to include both strong and relatively weak sockets. Subsequently, an alignment of related receptor sequences (*22*) was used to determine which sockets were most conserved and thus most likely to contribute significantly to helix−helix packing stability. Finally, sockets in which the knob was Ala were eliminated, yielding a library of conserved sockets with knobs all larger than Ala.

Creation and Isolation of Mutant Aspartate Receptors. Site-directed mutagenesis was performed as previously described (*28*) using the PCR-based QuickChange mutagenesis kit to engineer point mutations into the *Salmonella typhimurium* aspartate receptor gene in plasmid pSF6 (*40*). Mutated plasmids were transformed into *E. coli* strain RP3808 lacking the major endogenous receptors and other pathway components and expressed, and then receptor-containing membranes were isolated, quantitated, and stored as previously described (*23*) except that the EDTA[1] concentration was reduced from 10 to 0.1 mM in the high-salt buffer. The final membranes were resuspended at a receptor monomer concentration of ~50 μM in EDTA-free final buffer [20 mM sodium phosphate (pH 7.0) with NaOH, 10% glycerol, and 0.5 mM phenylmethanesulfonyl fluoride].

Oxidation of Receptors To Form Disulfide Bonds. Disulfide formation reactions were conducted for receptor-containing membranes (6 μM receptor dimer) in buffer A [50 mM Tris (pH 7.2) with HCl, 5 mM $MgCl_2$, and 160 mM KCl]. Reactions were initiated via addition of the redox catalyst Cu(II)(1,10-phenanthroline)$_3$ (0.2 or 2 mM as indicated) in the presence of ambient dissolved oxygen (200 μM). No EDTA was used to buffer the catalyst. Parallel reactions including the reducing agent DTT (75 mM) instead of redox catalyst were conducted to enable comparisons between the fully disulfide linked and fully reduced states. All reaction mixtures were incubated for 20 min at 37 °C, then were placed on ice, and immediately divided and reconstituted with CheA and CheW (both Cysless) for kinase assays, or with CheR for methylation assays (assays described below). Part of each sample was quenched by mixing with 2× Laemmli nonreducing sample buffer (235 mM Tris pH 6.8, 50% (w/v) glycerol, 7% SDS, 0.07% bromophenol blue) containing 10 mM EDTA and 40 mM *N*-ethylmaleimide (NEM) and was immediately heated to 95 °C for 1 min to promote unfolding; then products were resolved by Laemmli sodium dodecyl sulfate−polyacrylamide gel electrophoresis (SDS−PAGE) and quantitated by densitometry of the Coomassie-stained protein bands as previously described (*20*, *23*). The oxidation conditions used herein were considerably stronger than those used in early studies (*33*−*37*), enabling disulfide formation to be driven to completion. These stronger oxidation conditions were made possible due to the use of Cysless CheA and CheW proteins (*28*): in the past, such oxidation conditions were not possible because they interfered with kinase assays employing wild-type CheA and CheW, both of which contain native Cys residues. CheR also contains native Cys residues but is less sensitive to oxidation: membranes exposed to the strongest oxidation conditions (2 mM catalyst) inhibited maximum CheR activity approximately 25%. To correct for this effect, CheR activities were normalized to that measured for wild-type (WT) receptor membranes treated with the same oxidation conditions.

Receptor Activity Assays. Mutant receptors were assessed for their ability to regulate chemotaxis in vivo by expressing each receptor in *E. coli* strain RP8611, a strain lacking the aspartate receptor, and then measuring cellular chemotaxis at 30 °C in a standard soft agar swim plate assay, using minimal medium containing 100 μM aspartate (*23*, *41*). Mutant receptors were assessed for their ability to activate and regulate CheA kinase by reconstituting receptor-containing, isolated membranes with purified CheA and CheW [Cysless constructs as previously described (*28*)] and then quantitating receptor-regulated kinase activity in the standard in vitro assay under conditions where the kinase activity of CheA is the rate-determining step in CheY phosphorylation (*28*). Mutant receptors were assessed for the ability of their adaptation sites to serve as substrates for methyl esterification by reconstituting receptor-containing membranes with purified CheR in the standard in vitro receptor methylation assay (*28*). Finally, mutant receptors which failed to significantly activate CheA kinase were tested for CheA binding using a previously described method (*16*).

Standard Deviation. Error ranges represent the standard deviation of the mean for $n \geq 3$.

RESULTS

Development of the Yin−Yang Model for Cytoplasmic Domain Signaling. We began our study by re-examining the engineered Cys residues and disulfide bonds previously proposed (*33*−*37*) to lock the cytoplasmic kinase control module of the full-length, membrane-bound aspartate receptor in its native on state that activates CheA kinase. Two technical advances achieved in recent years now make it possible to better characterize the effects of such modifications on receptor signaling. (i) The antisymmetric activity method more rigorously identifies modifications that stabilize the native receptor on or off signaling state (*19*). This method subjects modified receptors to both the receptor-coupled CheA kinase activity assay and the receptor-coupled CheR methylation activity assay. The receptor on state generates a positive signal in the kinase assay and a negative signal in the methylation assay, while the off state yields the opposite results. These antisymmetric activity patterns yield unambiguous identification of the native signaling states. (ii) The availability of Cysless CheA and CheW proteins (*28*) now enables the use of stronger oxidation conditions to drive engineered disulfide bonds toward completion, thereby allowing more rigorous analysis of their effects on receptor-regulated kinase activity. Oxidation of native proteins (aspartate receptor, CheA, CheW, and CheY) prior to the kinase assay leads to inhibition of kinase activity (K. E. Swain and J. J. Falke, data not shown), presumably due to oxidative damage to native Cys residues in CheA and/or CheW since receptor and CheY both lack Cys residues. By contrast, even strong oxidation conditions yield little inhibition of kinase assays employing Cysless CheA and CheW (K. E. Swain and J. J. Falke, data not shown). Turning to the methylation assay, we found the native CheR employed herein contains native Cys residues, but inhibition of this enzyme by the strong oxidation chemistry is minor and easily identified by appropriate controls (see Materials and Methods). Overall, then, most engineered pairs of receptor Cys residues can be oxidized virtually completely to disulfide prior to functional analysis in both the kinase and methylation assays.

[1]Abbreviations: NEM, *N*-ethylmaleimide; DTT, dithiothreitol; EDTA, ethylenediaminetetraacetic acid; Cu-Phen$_3$, Cu(II) [1,10-phenanthroline]$_3$.

We have employed these two technical advances to carefully reexamine the relevant Cys and disulfide modifications in the kinase control module. As positive controls, a total of six signal-retaining, lock-on, and lock-off disulfides previously identified in the periplasmic and transmembrane regions (*40*, *42*) were also included. These control disulfides each form efficiently under the relatively mild oxidation conditions employed previously, and their functional effects have been analyzed by multiple activity assays (*40*, *42*), ensuring their suitability as positive controls in this study. The new findings for the positive control disulfides, summarized in Table S1 of the Supporting Information, indicate that the new methods correctly identify the different functional effects of receptor modifications. Application of these methods to modifications located in the kinase control module confirms that 16 previously identified lock-on modifications, namely, 11 Cys substitutions and five disulfide bonds, do indeed trap the receptor in the on state as operationally defined both by (i) high, aspartate-insensitive kinase activity and (ii) low, aspartate-insensitive receptor methylation rates (see Table S1 of the Supporting Information and Figure 4A). In addition, the new findings reveal a previously unknown lock-on disulfide in the adaptation region (Table S1 of the Supporting Information). Overall, a striking spatial segregation of lock-on modifications is observed: 9 of the 11 lock-on Cys residues are located in the protein interaction region, while 5 of the 6 lock-on disulfide bonds are located in the adaptation region (Figure 4A).

The observation that lock-on Cys residues are highly concentrated in the protein interaction region, while lock-on disulfides are located primarily in the adaptation region, has led us to propose the yin−yang hypothesis. In this model, signals are transmitted through the four-helix bundle of the kinase control module via antisymmetric changes in helix−helix packing that occur in a concerted fashion in the adaptation and protein interaction regions. In the adaptation region, stronger helix interactions within the four-helix bundle are proposed to stabilize the receptor on state, and weaker interactions are proposed to stabilize the off state. This model explains the observation that multiple lock-on disulfides can be generated in the adaptation region, each of which covalently stabilizes helix−helix contacts and constitutively favors the on state. In addition, the model is consistent with observation that electrostatic repulsion between multiple negative charges in the adaptation region destabilizes helix−helix packing and favors the off state, while covalent modification (methylation or amidation) of the adaptation Glu residues reduces electrostatic repulsion, stabilizes helix−helix packing, and favors the on state (*23*). In the protein interaction region, the yin−yang model proposes that helix−helix interactions exhibit the opposite functional effects; therefore, stronger helix−helix contacts within the protein interaction bundle stabilize the receptor off state, and weaker contacts stabilize the on state. This feature explains the observation that multiple Cys substitutions located at helix−helix interfaces in the protein interaction region, which presumably weaken local packing interactions, lock the receptor in the on state. The yin−yang hypothesis is testable, as illustrated by studies described below.

While our reanalysis has confirmed the previous functional classifications of 22 control and experimental receptor modifications, it has also revealed that several modifications were incorrectly classified in previous studies. Notably, the four adaptation region disulfide bonds previously assigned as signal-retaining, and thus believed to retain normal receptor on−off switching (G271C−G271C′, S272C−S272C′, A304C−A304C′, and G467C−G467C′) (*33*, *36*), are not confirmed (Table S1 of the Supporting Information). The weaker oxidation conditions employed by previous studies did not drive these disulfides to completion, leading to the misidentification. Here we were able to drive three of the disulfides nearly to completion, yielding altered functional classifications (G271C−G271C′, lock-on; S272C−S272C′, dead; A304C−A304C′, dead; where dead is a highly perturbed state characterized by loss of activity in both assays, presumably due to adverse structural effects). The fourth disulfide could not be formed efficiently even with the stronger oxidation conditions (G467C−G467C′). Since there are no longer any known signal-retaining disulfides in the adaptation region, there is no evidence to support the previous suggestion that the conformational change in this region is small enough to be accommodated by the range of disulfide bond conformational flexibility (*33*, *36*). However, given the extensive core hydrophobic interactions throughout most regions of the kinase control module, it is likely that the four-helix bundle remains largely formed throughout the three regions of the module in both signaling states, which limits the magnitude of helix−helix packing changes during on−off switching. Local defects in four-helix bundle structure remain possible, and structural studies of thermophillic receptors suggest that local defects may indeed occur (*24*−*26*).

Strategy for Testing the Yin−Yang Model by Weakening Sockets at Helix−Helix Interfaces. To test the yin−yang model for signaling in the kinase control module, a strategy to weaken local helix−helix interactions and to determine the resulting effects on receptor signaling state was devised. As is typical for antiparallel four-helix bundles, the helix−helix interactions in the kinase control module are stabilized by local "socket" structural elements, in which a "knob" residue on one helix inserts into a cavity formed by four "hole" residues on an adjacent helix (*38*, *39*). The component helices exhibit the usual repeating heptad pattern in which positions **a** and **d** are buried, positions **b**, **c**, and **f** are exposed, and positions **e** and **g** are interfacial. The knob residues are located at positions **a** and **d**, while the hole residues are typically at positions **a**, **d**, **e**, and **a** or positions **d**, **g**, **a**, and **d**, respectively. The strongest sockets possess large, hydrophobic knob and hole residues, although a broad range of socket strengths is created by the diversity of residues found at both knob and hole positions. In general, a selected socket can be weakened by introduction of a small side chain at one or more of its positions, thereby decreasing the surface area of knob-in-hole contacts.

Here we test the yin−yang model by introducing point mutations that replace selected knob side chains with the smaller Ala side chain. For the sake of simplicity, these mutations are each termed a "knob truncation". Each knob truncation weakens a socket and thus destabilizes a local helix−helix interaction. Subsequently, the effect of each knob truncation on the receptor signaling state is determined using the antisymmetric activity assay. The yin−yang model predicts that knob truncations in the adaptation and protein interaction regions will often generate lock-off and lock-on receptors, respectively. An example is illustrated in Figure 2, where a hydrophobic knob (L415) in the known structure of the protein interaction region contacts a hydrophobic hole (I359′, I362′, I363′, and I366′) in the opposite subunit. Truncation of the Leu to Ala is predicted to significantly reduce the contacts of the knob with its hole residues and weaken the socket. Since the mutation would weaken helix−helix packing in the protein interaction region, the yin−yang model predicts an

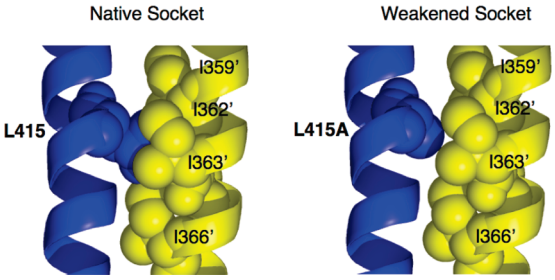

FIGURE 2: Method for analyzing the effects of local helix−helix interactions. Helix−helix packing in four-helix bundles is stabilized by socket interactions in which a knob side chain inserts into a hole formed by four side chains on an adjacent helix (*38*, *39*). Thus, to locally reduce the strength of helix−helix packing, in general one can truncate the side chain of a selected knob to Ala, thereby weakening the knob-in-hole packing of a native, interhelix socket. Shown is a representative socket (left) in which L415 is the knob that inserts into a hole comprised of I359′, I362′, I363′, and I366′ on an adjacent helix provided by the other subunit. Truncating the knob side chain from Leu to Ala, a mutation termed a knob truncation, significantly decreases the surface area of the knob−hole contacts (right).

increased probability that the mutant receptor would be locked in its kinase-activating, methylation-inhibiting on state.

To select a library of suitable knob side chains for truncation to Ala, SOCKET by Walshaw and Woolfson (*38*, *39*) was used to predict the strongest sockets in the published structural model for the kinase control module (*8*, *17*) (see Materials and Methods). Subsequently, an alignment of related receptor sequences was used to determine which sockets were most conserved, and thus most likely to contribute significantly to helix−helix packing stability (*22*). Finally, sockets in which the knob was already Ala were eliminated. This procedure yielded the library of 32 conserved aspartate receptor sockets targeted for knob truncation, as summarized in Table 1. The library included 16 sockets in the adaptation region, 8 in the coupling region, and 8 in the protein interaction region. Some knobs insert into a hole on the adjacent helix in the same subunit, while others insert into a hole on an adjacent helix in the other subunit, yielding intra- and intersubunit sockets, respectively (in Table 1 the hole residues of intersubunit sockets are indicated by a prime). All but four of the 32 knobs are hydrophobic, and the four exceptions are each neutral, hydrogen-bonding side chains (Ser, Asn, and Gln) that insert into holes containing at least one other hydrogen-bonding side chain. In some cases, a knob residue is also a hole residue for a different conserved socket (Table 1); in principle, truncation of such a residue to Ala will thus weaken two sockets simultaneously and thereby have an even greater destabilizing effect on local helix−helix interactions.

It should be noted that while a high-resolution crystal structure of a receptor cytoplasmic domain fragment accurately defines the structures of the coupling and protein interaction regions, the adaptation region is perturbed in this crystal structure by the truncation of its helices and by non-native crystal packing interactions (PDB entry 1QU7) (*8*, *17*). Thus, the SOCKET analysis utilized the crystal structure coordinates for the coupling and protein interaction regions but for the adaptation region instead used the coordinates provided by a molecular model of the full-length receptor (*8*, *17*). The structure of the adaptation region in the latter full receptor model is consistent with chemical studies of adaptation region structure in the full-length, membrane-bound receptor (*8*, *17*, *33*, *34*). Finally, the fact that each of the 32 selected sockets is conserved provides strong support for their correct identification in all three regions of the kinase control module.

Construction of a Weakened-Socket Receptor Library. To create a library of mutant aspartate receptors possessing weakened sockets in the kinase control module, PCR site-directed mutagenesis of the aspartate receptor gene *tar* was used to introduce Ala substitutions at the 32 selected knob positions. The resulting point mutations were confirmed by DNA sequencing. Mutant receptors were expressed in an *E. coli* strain lacking all major components of the chemotaxis pathway, including the adaptation enzymes (CheB and CheR). The absence of adaptation enzymes ensured that each mutant receptor population possessed identical adaptation sites and thus was homogeneous.

When expressed, 28 of the 32 weakened-socket mutants were stable, membrane-incorporated receptors accounting for 9 ± 1 to $14 \pm 1\%$ of the total membrane protein (TMP). These 28 mutants assemble into trimers of dimers since they activate and/or bind CheA at near-normal levels (see below). The four remaining mutants located in the adaptation (N317A, V471A, and V475A) and protein interaction (V401A) regions exhibited very low yields of membrane-associated receptor ($< 1\%$ TMP) insufficient for further study (Table 1). The strong effects of knob truncations at these four positions suggest the corresponding sockets may play an important role in assembly or stability.

Effects of Weakened Sockets on Receptor-Regulated CheA Kinase Activity. To analyze the effects of the 28 remaining weakened sockets on the receptor signaling state, the behavior of each modified receptor was tested in the antisymmetric activity assay (*19*). Of special interest are modifications that lock the receptor in its on or off state. In the kinase assay, wherein the receptor is reconstituted with CheA and CheW to generate the functional, membrane-bound signaling complex, lock-on modifications trap the signaling complex in the kinase activating state such that it becomes insensitive to attractant binding. By contrast, lock-off modifications trap the complex in the kinase-inhibiting state.

Table 1 and Figure 3A summarize the effects of weakened sockets on receptor-regulated CheA kinase activity. Strikingly, the effects can be grouped into three distinct classes (Figure 3A). One class (V268A, Q296A, T303A, V447A, and V510A) exhibits wild-type-like kinase activity, including nearly complete inhibition by attractant aspartate. A second class (I359A, I363A, V397A, L404A, I415A, I419A, V426A, V450A, and M454A) exhibits potential lock-on character because even high, nonphysiological levels (1 mM) of aspartate do not fully inhibit kinase activity; instead, the remaining kinase activity is at least 4-fold that of the wild-type receptor in its aspartate-occupied state. A third class (V265A, I282A, N286A, L300A, V314A, M349A, I352A, I366A, L376A, I457A, S461A, I468A, M478A, and F513A) exhibits potential lock-off activity, since little or no kinase activation is observed even in the absence of aspartate.

Alternatively, the loss of kinase activation observed for the third class of weakened sockets could arise from failure of the mutant receptor to bind CheA kinase. Thus, the 15 modified receptors that exhibited kinase activities that were $\leq 25\%$ of that measured for the wild-type receptor were tested for normal complex formation with CheA and CheW in a pull-down assay (*16*, *28*). The resulting kinase binding data are summarized in Table 1. All 15 tested receptors bound at least 40% of the normal level of CheA, indicating that their low kinase activities were not due simply to the loss of CheA binding. By contrast, a negative control receptor (N379F) that fails to form trimers of

Table 1

knob (heptad position)	hole residue (n1, n4, n5, n8)	hole type[a]	kinase activity: without Asp	kinase activity: with Asp	methylation activity: without Asp	methylation activity: with Asp	kinase binding	measured effect[b]	swarm rate
			(A) Adaptation Region (amino acids 260−320, 461−520)						
WT			1.00 ± 0.07	0.04 ± 0.02	1.00 ± 0.03	3.08 ± 0.19	1.00 ± 0.13	WT	1.00 ± 0.12
V265A (**a**)	510 (V, F, R, S)	4	0.02 ± 0.01	0.01 ± 0.01	0.21 ± 0.03	0.34 ± 0.02	0.41 ± 0.03	dead	0.03 ± 0.02
V268A (**d**)	506′ (L, A, V, F)	4	0.44 ± 0.05	0.05 ± 0.01	0.15 ± 0.01	0.18 ± 0.02	−	perturbed	0.94 ± 0.19
I282A (**d**)	492′ (S, A, A, L)	4	0.02 ± 0.01	0.01 ± 0.01	2.22 ± 0.06	3.44 ± 0.01	1.06 ± 0.03	lock-off	0.02 ± 0.02
N286A (**a**)	489 (V, S, A, A)	2	0.02 ± 0.01	0.01 ± 0.01	3.15 ± 0.13	3.84 ± 0.11	1.23 ± 0.01	lock-off	0.07 ± 0.02
Q296A (**d**)	478′ (M, V, T, N)	2	1.13 ± 0.02	0.05 ± 0.01	0.76 ± 0.06	3.46 ± 0.07	−	SR	1.68 ± 0.21
L300A (**a**)	475 (V, M, D, T)	4	0.02 ± 0.01	0.01 ± 0.01	3.97 ± 0.16	3.23 ± 0.08	1.08 ± 0.09	lock-off	0.50 ± 0.08
T303A (**d**)	471′ (V, A, V, M)	4	1.03 ± 0.08	0.01 ± 0.01	0.44 ± 0.02	1.31 ± 0.14	−	perturbed	0.02 ± 0.03
V314A (**a**)	461 (S, Q, S, I)	2	0.02 ± 0.01	0.01 ± 0.01	1.84 ± 0.06	2.70 ± 0.22	0.97 ± 0.08	lock-off	0.01 ± 0.02
(N317A)(**d**)	459′ (I, A, S, Q)	2						(low yield)	
S461A (**a**)	314 (V, N, A, A)	2	0.02 ± 0.01	0.01 ± 0.01	1.95 ± 0.14	2.53 ± 0.13	1.22 ± 0.08	lock-off	1.04 ± 0.05
I468A (**a**)	307 (M, L, T, V)	2	0.02 ± 0.01	0.01 ± 0.01	1.62 ± 0.06	2.69 ± 0.19	0.83 ± 0.01	lock-off	0.01 ± 0.02
(V471A) (**d**)	305′ (T, S, M, L)	2						(low yield)	
(V475A) (**a**)	302 (L, T, A, M)	4						(low yield)	
M478A (**d**)	296′ (Q, A, L, T)	4	0.02 ± 0.01	0.01 ± 0.01	2.16 ± 0.18	3.48 ± 0.37	1.27 ± 0.10	lock-off	0.02 ± 0.02
V510A (**a**)	265 (V, V, R, S)	4	0.65 ± 0.12	0.00 ± 0.01	0.27 ± 0.02	0.57 ± 0.06	−	perturbed	0.78 ± 0.17
F513A (**d**)	261′ (L, T, V, V)	4	0.05 ± 0.01	0.01 ± 0.01	0.04 ± 0.01	0.04 ± 0.01	1.15 ± 0.06	dead	0.06 ± 0.03
N379F	(disrupts trimer)		0.01 ± 0.01	0.01 ± 0.01	2.96 ± 0.10	4.50 ± 0.16	0.06 ± 0.02	dead	0.01 ± 0.03
			(B) Coupling Region (amino acids 321−362, 420−460)						
WT			1.00 ± 0.07	0.04 ± 0.02	1.00 ± 0.03	3.08 ± 0.19	1.00 ± 0.13	WT	1.00 ± 0.12
M349A (**a**)	345′ (V, T, M, I)	1	0.01 ± 0.01	0.00 ± 0.01	1.07 ± 0.07	2.68 ± 0.16	1.18 ± 0.01	perturbed	0.04 ± 0.03
I352A (**d**)	422 (S, R, V, G)	NS	0.00 ± 0.01	0.00 ± 0.01	0.16 ± 0.01	0.17 ± 0.02	0.40 ± 0.01	dead	1.25 ± 0.21
I359A (**d**)	415 (I, L, I, S)	4	0.90 ± 0.06	0.12 ± 0.01	0.54 ± 0.03	2.00 ± 0.18	−	SR	1.33 ± 0.17
V426A (**a**)	349 (M, I, A, S)	4	0.89 ± 0.09	0.26 ± 0.05	0.30 ± 0.02	1.00 ± 0.10	−	SR	1.32 ± 0.04
V447A (**a**)	328 (A, A, S, A)	4	0.82 ± 0.07	0.00 ± 0.01	1.50 ± 0.11	3.30 ± 0.14	−	SR	0.85 ± 0.03
V450A (**d**)	324′ (A, L, A, A)	1	0.72 ± 0.10	0.18 ± 0.03	0.48 ± 0.04	1.40 ± 0.05	−	SR	1.13 ± 0.18
M454A (**a**)	321′ (A, A, S, A)	1	0.96 ± 0.11	0.10 ± 0.02	0.56 ± 0.03	2.02 ± 0.11	−	SR	1.22 ± 0.17
I457A (**d**)	317 (N, N, A, A)	NS	0.00 ± 0.01	0.00 ± 0.01	0.20 ± 0.02	0.21 ± 0.01	1.33 ± 0.01	dead	0.30 ± 0.02
N379F	(disrupts trimer)		0.01 ± 0.01	0.01 ± 0.01	2.96 ± 0.10	4.50 ± 0.16	0.06 ± 0.02	dead	0.01 ± 0.03
			(C) Protein Interaction Region (amino acids 363−419)						
WT			1.00 ± 0.07	0.04 ± 0.02	1.00 ± 0.03	3.08 ± 0.19	1.00 ± 0.13	WT	1.00 ± 0.12
I363A (**a**)	412 (A, I, R, I)	1	1.20 ± 0.07	1.06 ± 0.05	0.06 ± 0.01	0.33 ± 0.05	−	lock-on	0.01 ± 0.02
I366A (**d**)	408 (S, A, A, I)	3	0.02 ± 0.01	0.01 ± 0.01	0.39 ± 0.12	0.76 ± 0.01	0.42 ± 0.05	dead	0.21 ± 0.06
L376A (**d**)	397′ (V, E, V, L)	4	0.03 ± 0.01	0.02 ± 0.01	0.28 ± 0.03	0.57 ± 0.06	0.79 ± 0.08	dead	0.21 ± 0.08
V397A (**d**)	376′ (L, N, A, E)	2	0.25 ± 0.02	0.16 ± 0.01	0.04 ± 0.01	0.07 ± 0.01	1.01 ± 0.09	lock-on	0.01 ± 0.02
(V401A) (**d**)	375 (T, L, A, A)	4						(low yield)	
L404A (**d**)	369′ (I, Q, T, L)	2	0.49 ± 0.03	0.33 ± 0.02	0.07 ± 0.01	0.31 ± 0.03	−	lock-on	0.74 ± 0.012
I415A (**d**)	359′ (I, I, I, I)	3	0.88 ± 0.10	0.68 ± 0.06	0.07 ± 0.01	0.28 ± 0.03	−	lock-on	0.02 ± 0.02
I419A (**a**)	356 (S, I, A, I)	2	0.95 ± 0.08	0.91 ± 0.01	0.14 ± 0.02	0.45 ± 0.05	−	lock-on	0.02 ± 0.02
N379F	(disrupts trimer)		0.01 ± 0.03	0.01 ± 0.01	2.96 ± 0.10	4.50 ± 0.16	0.06 ± 0.02	dead	0.01 ± 0.03

Abbreviations. [a]NS, not standard. [b]SR, signal-retaining; perturbed, inactive in one assay; dead, inactive in two assays; (low yield), < 1% total membrane protein.

dimers (*43*) exhibited no detectable kinase activity and yielded only 6% of the normal level of CheA binding, confirming that the assay successfully detects poor CheA binders.

Effects of Weakened Sockets on Receptor-Regulated CheR Methylation Activity. To positively identify modifications that trap the native receptor on and off states, the antisymmetric activity assay also measures the effect on receptor-regulated methylation activity in the reconstituted receptor−CheR complex (*19*). Lock-on modifications trap the signaling complex in the state exhibiting low methylation activity, such that addition of attractant fails to trigger the native increase in the receptor methylation rate. By contrast, lock-off modifications trap the complex in the state exhibiting high receptor methylation activity, even in the absence of attractant.

Table 1 and Figure 3B summarize the effects of weakened sockets on receptor-regulated CheR methylation activity. Again, the effects can be grouped into three different classes (Figure 3B). One class (Q296A, M349A, I359A, V447A, and M454A) exhibits wild-type-like methylation activity, yielding a methylation rate within the range of that of WT ± 50%, as well as near-normal attractant regulation in which aspartate triggers a 2−4-fold increase in methylation rate. A second class (I282A, N286A, L300A, V314A, S461A, I468A, and M478A) exhibits potential lock-off character, since high levels of methylation are observed even in the absence of aspartate. A third class (V265A, V268A, T303A, I352A, I363A, I366A, L376A, V397A, L404A, I415A, I419A, V426A, V450A, V510A, and F513A) exhibits potential lock-on activity, since low levels of methylation are observed with

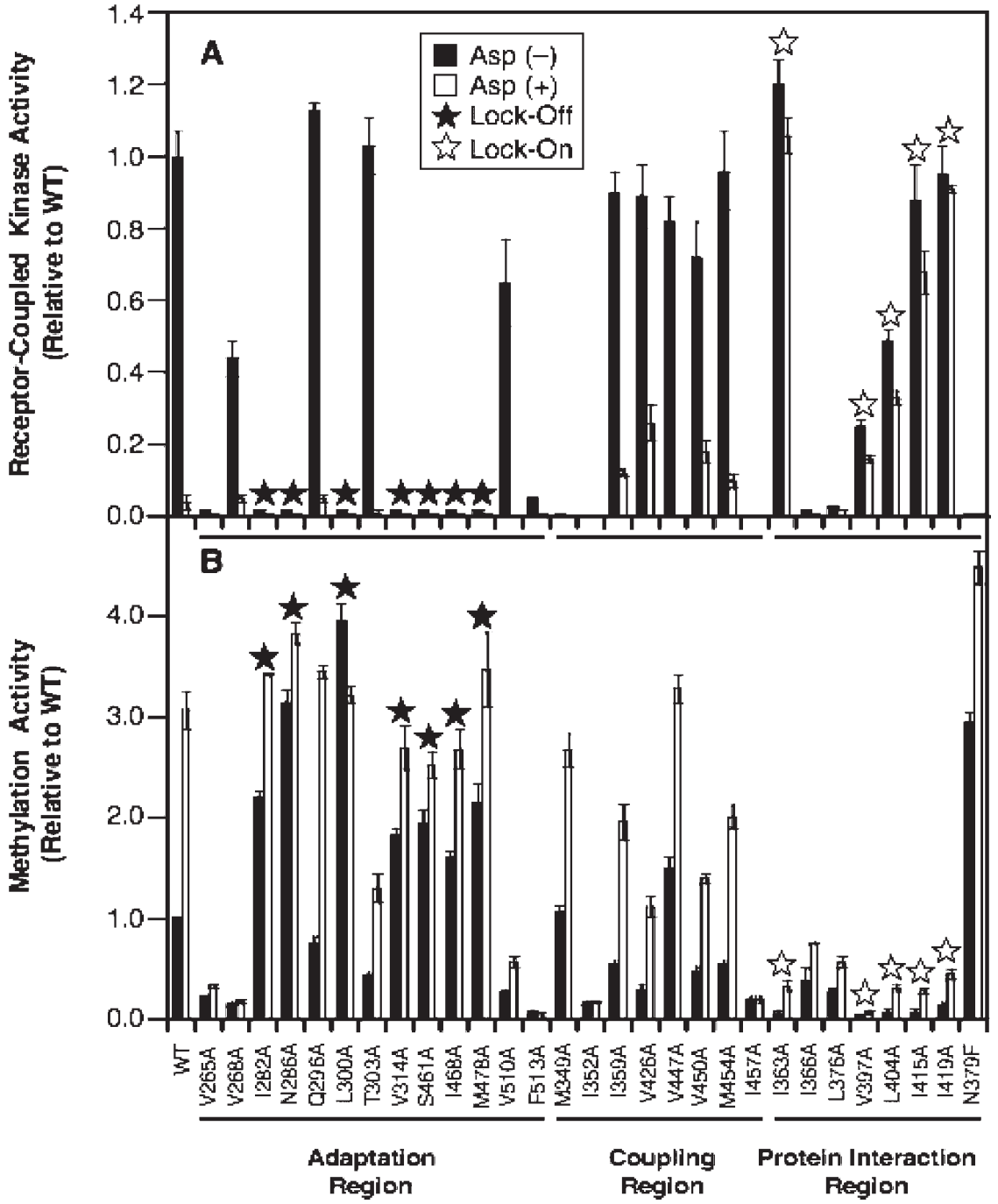

FIGURE 3: Effects of weakened sockets on receptor function in vitro. (A) Effects of knob truncations (defined in Figure 2) on receptor-regulated kinase activity in the reconstituted receptor−CheA−CheW signaling complex. Shown are CheA kinase activities for signaling complexes containing each knob truncation mutant in both the apo (■) and attractant-occupied [1 mM Asp (□)] states. All kinase activities are normalized to that of the signaling complex containing the apo wild-type receptor. Notably, a high percentage of knob truncations in the adaptation region inhibit kinase activity, while a high percentage in the protein interaction region prevent normal attractant inhibition of kinase activity. (B) Effects of knob truncations on receptor methylation rates in the reconstituted receptor−CheR complex. Shown are rates of adaptation site methyl esterification by CheR, both in the apo (■) and attractant-occupied [1 mM Asp (□)] states. All rates are normalized to that of the apo wild-type receptor−CheR complex. A high percentage of knob truncations in the adaptation region led to high methylation rates even in the absence of attractant, while in the protein interaction region, the methlation rates are typically low in both the absence and presence of attractant. In addition to the 28 knob truncation mutants, each panel also includes the wild-type (WT) receptor and a control receptor (N379F), which does not form the trimer of dimers (*43*) and thus is inactive in the kinase and live cell assays but is methylated faster than the wild type because of the increased accessibility of the adaptation sites to CheR. Knob truncations that are operationally defined (see the text) as signal-locking, either lock-on (☆) or lock-off (★), are denoted.

little or no activation triggered by a high concentration (1 mM) of aspartate.

Weakened Sockets That Trap the Receptor On and Off States, and Effects on Chemotaxis. Using the standard antisymmetric activity approach, the combined results of the in vitro kinase and methylation assays identify a set of 12 weakened sockets that trap the receptor (*44*) in one of two states, operationally defined as the on or off state, as summarized in Table 1 and Figures 3 and 4. Presumably, these states correspond to the on and off states exhibited by the native, two-state receptor (*44*).

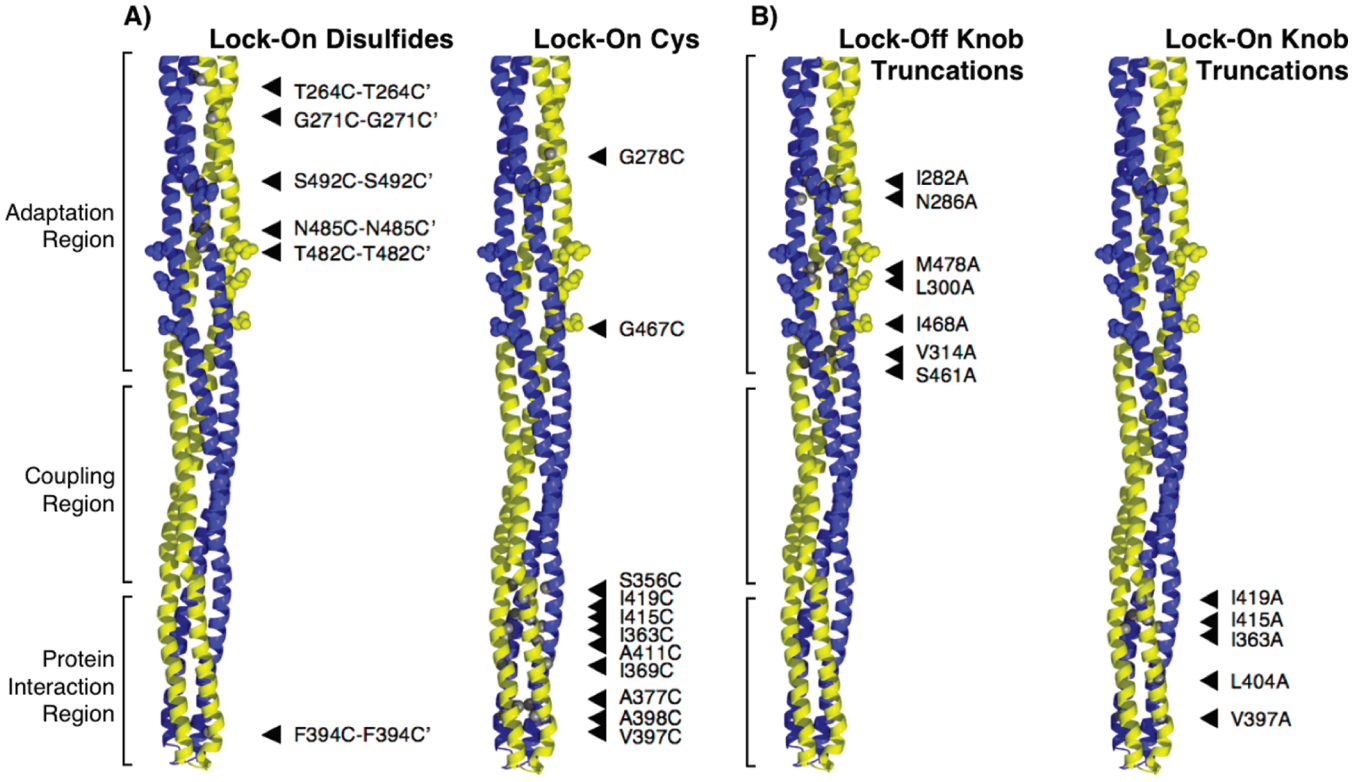

FIGURE 4: Locations of lock-on and lock-off modifications in the kinase control module. Shown is the kinase control module of a single receptor homodimer (*1*), with the two subunits distinguished by color (blue and gold). Each arrowhead indicates the position of a signal-locking modification (small spheres) in the homodimer, as identified by the antisymmetric activity assay (see the text). Lock-on modifications are operationally defined by high rates of receptor-regulated CheA kinase activity, even in the presence of attractant that normally turns the kinase off, as well as low CheR methylation activity regardless of the attractant concentration. Lock-off modifications are defined by low rates of receptor-regulated CheA kinase activity, and high rates of CheR methylation activity, regardless of the attractant concentration. (A) Locations of lock-on disulfide bonds and lock-on Cys substitutions, first described in previous studies (*33*−*37*) and reconfirmed here using more rigorous methods. The lock-on disulfides covalently stabilize helix−helix packing and are located predominantly in the adaptation region, while the lock-on Cys substitutions likely weaken helix−helix packing and are predominantly located in the protein interaction region. (B) Locations of lock-on and lock-off knob truncations, which are clustered in the protein interaction and adaptation regions, respectively. These modifications illustrate the opposite effects that weaker knob-in-holes packing has on the receptor signaling state in the two different regions.

Five weakened sockets, all in the protein interaction region (I363A, V397A, L404A, I415A, and I419A), simultaneously yield relatively high kinase activity and low methylation activity, even in the presence of saturating attractant, indicating that these sockets trap the receptor in the on state. Seven weakened sockets, all in the adaptation region (I282A, N286A, L300A, V314A, S261A, I468A, and M478A), yield low kinase activity and high methylation activity irrespective of attractant level, indicating these sockets trap the off state. By contrast, while most weakened sockets in the adaptation and protein interaction regions have large effects on kinase and/or methylation activities, in the coupling region most weakened sockets have only minor effects on both assays and no lock-on or lock-off modifications are observed in this region (Table 1 and Figure 3).

Analysis of the effects of weakened sockets on receptor-regulated chemotaxis in live cells, summarized in Table 1, reveals that lock-on and lock-off modifications generally block chemotaxis as expected. In four of five cases, the lock-on modifications virtually eliminate receptor-regulated live cell chemotaxis. Similarly, in five of seven cases, the lock-off modifications block live cell chemotaxis. The simplest explanation for these strong effects on chemotaxis is that the signal-locking character of these nine weakened sockets is retained in vivo, thereby preventing the receptor on−off switching that is essential for pathway function. The three remaining exceptions (L300A, S461A, and L404A) exhibit signal locking character in vitro but display more normal function in vivo, suggesting that in live cells the native CheB−CheR adaptation system (absent in the in vitro experiments) can partially repair the signal locking defects of these three weakened sockets. Such repairs are not surprising, since it is well-established that the adaptation system can correct certain receptor defects and thereby maintain pathway function (*33*, *35*, *36*, *40*).

DISCUSSION

Overall, this study illustrates the usefulness of the knob truncation scan in testing the role of helix−helix interactions in protein function and mechanism. This new method targets the knob side chains of conserved sockets that stabilize helix−helix interactions via knob-in-holes packing (*38*, *39*). The method introduces a point mutation that shortens, or truncates, a given knob side chain to the smaller Ala, thereby reducing the number of knob-in-hole contacts and weakening the socket. The weakened socket, in turn, weakens the local helix−helix packing interaction. It is difficult to directly measure the effects of a given knob truncation on helix packing stability, and some knob truncations will likely not have the intended effects. Thus, a large library of knob truncations is essential to correctly identify spatial patterns. The functional effects of 28 knob truncations tested herein yield a striking spatial pattern that strongly supports the yin−yang hypothesis as illustrated in Figure 4. In the adaptation region, 7 of 13 knob truncations exhibit lock-off character that traps the receptor in its native kinase-inhibiting

state, both in the absence and in the presence of attractant. In the protein interaction region, 5 of 8 knob truncations exhibit lock-on character that stabilizes the native kinase-activating state, regardless of the attractant concentration. No signal locking mutations are detected in the coupling region. Thus, the opposing signaling polarities predicted by the yin−yang hypothesis for the adaptation and protein interaction regions are directly observed: weaker helix−helix packing in the adaptation region favors the receptor off state, while weaker packing in the protein interaction region favors the on state.

In both regions, signal locking mutations are observed at intrasubunit sockets and intersubunit sockets (Table 1). It follows that knob-in-hole interactions between helices in the same subunit, or between helices in different subunits of the same dimer, can both modulate yin−yang coupling and receptor on−off switching. Interestingly, the 28 knob truncations at conserved socket positions examined in detail here all retain significant CheA binding, indicating they all form the trimer-of-dimer oligomers needed to form stable receptor−CheA−CheW complexes (*1*, *51*, *43*, *16*), including the 14 locked-off or damaged mutants that are unable to activate CheA. Thus, in many cases, disruption of a single socket can shift the delicately tuned receptor signaling bias without destroying protein−protein structural interactions that likely involve multiple sockets or other contacts.

A group of previously characterized Cys substitutions and engineered disulfide bonds provide further evidence for the yin−yang signaling mechanism. Of the six known cytoplasmic, lock-on disulfide bonds, five are located in the 120-residue adaptation region where they covalently stabilize helix−helix interactions (*33*, *34*, *36*) (Figure 4A and Table S1 of the Supporting Information), supporting the yin−yang view that stabilization of helix packing in this region leads to kinase activation. Although they were characterized before we implemented our current antisymmetric activity assay and CheA kinase binding assay, Cys substitutions in the adaptation region also yield effects on kinase regulation consistent with yin−yang predictions (*33*, *36*). Cys substitutions at 18 buried positions in the adaptation region largely abolish kinase activity, while only two Cys substitutions at buried positions lock the receptor in the kinase-activating state (*33*, *36*). Of the 18 Cys substitutions that eliminate kinase activity, 10 are knob or hole residues at heptad position **a**, **d**, **e**, or **g** in one of the conserved, strong sockets identified in this study (Table 1). The eight remaining lock-off Cys substitutions are also located at heptad positions **a**, **d**, **e**, and **g** that may participate in sockets not satisfying the present proximity and conservation cutoffs (see Materials and Methods). Thus, most or all of the kinase-inhibiting Cys substitutions in the adaptation region weaken conserved sockets and thereby confirm the yin−yang prediction that weaker helix−helix interactions should favor the receptor off state. The two lock-on Cys substitutions in the adaptation region (Figure 4A) may also be explained by the yin−yang model, since both replace buried Gly positions with the more hydrophobic, less helix-destabilizing Cys side chain that may increase the stability of the adaptation four-helix bundle sufficiently to trap the on state.

In the 56-residue protein interaction region, a total of nine lock-on Cys substitutions have been identified which lock the receptor in its native kinase-activating on state exhibiting high kinase activity and low methylation activity (*34*, *35*, *37*) (Figure 4A). Of these nine lock-on Cys substitutions, seven are located at knob or hole positions in conserved, strong sockets

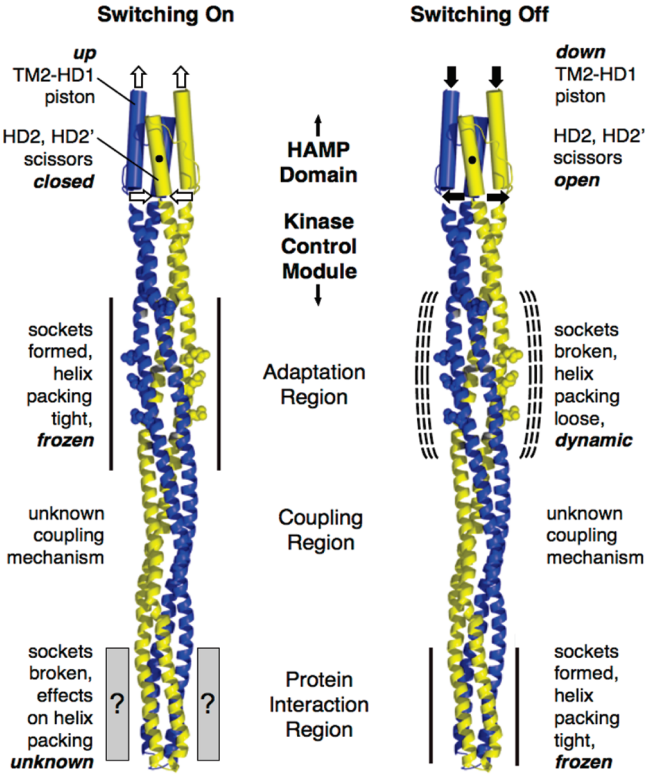

FIGURE 5: Conceptual basis of the yin−yang hypothesis. While the atomic structural−mechanical basis of the yin−yang signaling is not yet clear, the conceptual basis of the model is straightforward. Attractant binding to the periplasmic ligand binding domain triggers a transmembrane conformational change that is converted by the HAMP domain into a different type of conformational signal (*1*). Our current working model proposes that HAMP on−off switching triggers a scissors-type displacement of its C-terminal HD2−HD2′ helices that directly couple to the N-terminal helices of the kinase control module. In the kinase-activating on state, four-helix bundle packing is more stable (sockets formed) in the adaptation region, but less stable (sockets broken, at least partially) in the protein interaction region. The reverse is true in the kinase-inhibiting off state. Together with previous findings on helix dynamics in the adaptation region (*23*), these findings indicate that helix packing changes in this region yield a local frozen−dynamic transition (*47*) as illustrated. In the protein interaction region, no study of helix dynamics has yet been conducted, and it is not clear whether the loss of socket interactions (i) allows other stabilizing interactions to form, yielding a different stable conformation, or (ii) simply destabilizes the region, yielding a looser, more dynamic structure. The helix−helix packing in the coupling region is proposed to possess a significantly lower density of stabilizing sockets (*22*), and the location of this region indicates that it serves as a signal transmission element between the strongly coupled adaptation and protein interaction regions. The space-filling side chains represent the four adaptation Glu residues of each subunit, which can also drive yin−yang signaling via an electrostatic mechanism (*23*).

identified in this study (Table 1). It follows that the majority of these lock-on Cys substitutions weaken helix−helix packing by truncating knob or hole residues and thereby stabilize the kinase-activating state as predicted by the yin−yang hypothesis. In general, it was not possible to find engineered disulfide bonds in the protein interaction region with easily interpreted functional effects. In this region, all but two of the disulfide bonds tested in the antisymmetric activity assay disrupted native receptor structure, as revealed by simultaneously low kinase and methylation rates, or blocked kinase binding to the receptor, or both (K. E. Swain and J. J. Falke, unpublished observations). The only two exceptions were a signal-retaining disulfide and a lock-on

disulfide, both located near the hairpin turn at the extreme cytoplasmic tip of the receptor where they may stabilize structural features of the turn rather than helix−helix packing (Table S1 of the Supporting Information).

In contrast to the conserved sockets of the adaptation and kinase control regions, the conserved sockets of the 80-residue coupling region are not strongly tied to receptor function. As predicted by a bioinformatics analysis (*22*), helix−helix interactions in the coupling region appear to be weaker since even the strongest sockets in this region utilize residues that are predicted by socket theory to yield suboptimal knob-in-hole packing. Of 12 conserved sockets, four possess Ala knobs (and were thus excluded from this Ala substitution study) that generally yield weak sockets, while four others possess holes dominated by small hydrophobic or polar residues (Ala, Ser, and Asn) that also likely yield weak sockets. Of the eight knob truncations tested in the coupling region, only three strongly perturbed receptor function and none were signal-locking (Table 1B). This lack of signal-locking perturbations contrasted sharply with the other two regions: in the adaptation region, 54% of the knob truncations were lock-off, and in the protein interaction region, 62% were lock-on. Such findings are consistent with the hypothesis that the coupling region undergoes a low-energy conformational shift during signal transmission between the adaptation and protein interaction regions and possesses a low density of stable sockets to minimize the energetic barrier to this shift. We propose this region is essential to link the concerted yin−yang helix packing changes in the adaptation and protein interaction regions, and is not highly flexible and dynamic throughout since such extreme flexibility would be inconsistent with a coupling role. Thus, rather than the "flexible region", we term this the "coupling region". The region does contain the conserved Gly hinge, where yin−yang signals may alter the hinge angle during receptor on−off switching (*24*−*26*, *22*, *45*). Presumably, this hinge has evolved to enable tight yin−yang coupling.

Figure 5 summarizes our current working model for signal transduction through the receptor cytoplasmic domain, from the HAMP domain through the three regions of the kinase control module. Signals are initiated by two different types of input stimuli that drive receptor on−off switching (*1*, *6*, *23*, *46*). (i) Conformational signals triggered by attractant binding to the periplasmic ligand-binding domain cause a structural rearrangement of HAMP, which is in turn transmitted to the kinase control module (*1*, *6*). Our current working hypothesis proposes that attractant binding causes a scissors-type displacement of the C-terminal HD2 and HD2′ helices of the homodimeric HAMP about a pivot point (K. E. Swain and J. J. Falke, manuscript in preparation). As the scissors open, the displacement of the C-terminal ends of HD2 and HD2′, which are coupled to helices CD1 and CD1′ at the N-terminus of the kinase control module, strains the four-helix bundle packing in the adaptation region and favors the receptor off state (*23*). (ii) Electrostatic signals originating in the adaptation region, where a high density of anionic side chains lining the subunit interface generates electrostatic repulsion between helices, also weaken the packing of the adaptation region four-helix bundle and favor the receptor off state (*1*, *23*, *46*). During adaptation to a higher attractant concentration, neutralization of the receptor adaptation Glu side chains via methylation reduces the level of electrostatic repulsion between helices, thereby stabilizing helix−helix packing in the adaptation region and favoring the on state. Thus, in the adaptation region, attractant and adaptation signals generate opposing effects on the receptor signaling state by altering helix−helix interactions in opposite ways, as required for pathway function.

The yin−yang hypothesis further proposes that the coupling region faithfully transmits each change in helix packing from the adaptation region to the protein interaction region, where it triggers a helix packing change that is concerted but opposite in sign. The simplest interpretation of the knob truncation scan data is that conserved sockets in the adaptation region stabilize the receptor on state, while conserved sockets in the protein interaction region stabilize the off state. Thus, on signals stabilize sockets and their helix−helix interactions in the adaptation region but disrupt sockets and helix−helix interactions in the protein interaction region, while off signals have the reverse effects in the two regions. Such yin−yang coupling requires that the sockets in the two regions, as well as all other helix−helix interactions, be well balanced so that receptor signaling bias is maintained at an optimal level. Energetically, such a system employing competing socket interactions in two regions provides a significant advantage when low-energy signals (attractant binding, adaptation site modification) must trigger switching to a different signaling state, since the energetic cost of disrupting sockets in one region is largely balanced by the formation of sockets in the other region.

In structural and dynamical terms, the transition of the adaptation region between its on and off states appears to involve switching of the local four-helix bundle between a tightly packed, less mobile, "frozen" on state and a more loosely packed, more mobile, "dynamic" off state. Such a local frozen−dynamic transition is supported by evidence that (i) in the on state, local helix packing is stabilized by socket formation or by partial neutralization of repulsive charges at adaptation sites and (ii) in the off state, local helix packing is destabilized by the loss of socket interactions, or by an increased level of charge repulsion between helices (our data and ref *23*). Moreover, a signal-induced increase in local helix dynamics has been directly detected by Cys pairs introduced as collision monitors, which yield more rapid disulfide bond formation in the off state (*23*). This local frozen−dynamic transition differs from the global frozen−dynamic transition proposed by an early model for cytoplasmic domain on−off switching (*47*): in the latter model based on studies of cytoplasmic domain fragments, all three regions of the kinase control module simultaneously undergo the same frozen−dynamic transition described herein for the adaptation region. Our evidence, obtained for the full-length, membrane-bound receptor in its functional signaling complex, disfavors the global frozen−dynamic model since opposite changes in helix−helix packing are observed in the adaptation and protein interaction regions during on−off switching. These different findings for the cytoplasmic domain fragment and the full-length receptor could be explained by the loss of native helix packing constraints in the fragment construct. Such relatively unconstrained fragments may also be able to switch more easily into the on state, which would explain their ability to generate measurable activation of CheA kinase (*48*).

One of the two signaling states of the adaptation region may possess a recently described bulge in the four-helix bundle, observed in a crystal structure of a thermophillic adaptation region (*24*). The bulge forms when a symmetric, buried pair of Asn residues forms a bidentate hydrogen bond across the hydrophobic subunit interface within the local region containing the

adaptation sites. This pair of Asn residues (positions N485 and N485′ in the aspartate receptor) is widely conserved in chemotaxis receptors, including the chemoreceptors of *E. coli* and *S. typhimurium*. In the aspartate receptor, we have shown that a disulfide bond bridging the same two positions (N485C−N485C′) locks the receptor in the on state (*36*) (Table S1 of the Supporting Information). The lock-on disulfide is structurally similar to the Asn−Asn′ side chain interaction, suggesting that the latter is formed in the on state and broken in the off state, but this simple view could be misleading since the disulfide bond would generate closer helix−helix packing than the Asn−Asn′ interaction and thus is not a perfect structural match (*24*).

In the protein interaction region, it is not yet clear whether on−off switching triggers a local conformational change between two relatively stable states, or a local frozen−dynamic transition. When on-state signals disrupt local socket interactions, the region could adopt different stabilizing interactions yielding an alternate stable conformation (two-conformation model) or the local helix packing could become more dynamic (frozen−dynamic model). More work is needed to distinguish these possibilities. Moreover, the central mechanism of receptor-mediated kinase regulation remains unanswered: how does the switching of the protein interaction region between its two signaling states regulate CheA kinase activity? Here we propose a plausible but speculative hypothesis, based in part on a recent study of substrate domain mobility in free CheA kinase (*49*). In this hypothesis, the protein interaction region regulates the dramatic mobility of the substrate domain required for rapid collisions with the catalytic domain during autophosphorylation, and with CheY or CheB during phospho transfer. In the off state, the substrate domain is proposed to bind in a cleft where it interacts stably with both the protein interaction region and a distinct inhibitory site on the catalytic domain (*50*), thereby eliminating its mobility and inhibiting kinase activity. The on state of the protein interaction region is proposed to release the substrate domain from this inhibitory site, thereby restoring domain mobility and kinase activity.

The yin−yang model is likely to be relevant to a large superfamily of prokaryotic receptors: These receptors contain conserved adaptation, coupling, and protein interaction regions homologous to the aspartate receptor and likely share the same signal transduction mechanism (*22*). The model makes further testable predictions; for example, it is likely that the signaling effects of socket modifications will be additive, so that multiple socket mutations with partial lock-on (or lock-off) character will generate signaling states that are more fully locked-on (or -off). Such signal-locking socket modifications may well be useful in future biophysical studies of the mechanical basis for the remarkable coupling between the adaptation and protein interaction regions. By contrast, multiple socket mutations with opposite character should cancel each other out; for example, simultaneous incorporation of socket-weakening mutations in the adaptation and protein interaction regions is predicted to have little effect on receptor signaling state. Future studies will continue to investigate the nature of receptor on−off switching in the active, membrane-bound signaling complex.

NOTE ADDED AFTER ASAP PUBLICATION

There were errors in Table 1 in the version that posted ASAP on September 11, 2009. These have been fixed in the version that posted ASAP on September 29, 2009.

ACKNOWLEDGMENT

We gratefully acknowledge Prof. Robert Hodges (University of Colorado Health Sciences Center, Denver, CO) for helpful discussions about socket structure and stability and Dr. Annette Erbse for helpful comments on the manuscript.

SUPPORTING INFORMATION AVAILABLE

Summary of the functional effects of interhelix disulfide bonds (Table S1). This material is available free of charge via the Internet at http://pubs.acs.org.

REFERENCES

1. Hazelbauer, G. L., Falke, J. J., and Parkinson, J. S. (2008) Bacterial chemoreceptors: High-performance signaling in networked arrays. *Trends Biochem. Sci. 33*, 9–19.
2. Tindall, M. J., Porter, S. L., Maini, P. K., Gaglia, G., and Armitage, J. P. (2008) Overview of mathematical approaches used to model bacterial chemotaxis I: The single cell. *Bull. Math. Biol. 70*, 1525–1569.
3. Bardy, S. L., and Maddock, J. R. (2007) Polar explorations. Recent insights into the polarity of bacterial proteins. *Curr. Opin. Microbiol. 10*, 617–623.
4. Baker, M. D., Wolanin, P. M., and Stock, J. B. (2006) Signal transduction in bacterial chemotaxis. *BioEssays 28*, 9–22.
5. Bourret, R. B., and Stock, A. M. (2002) Molecular information processing: Lessons from bacterial chemotaxis. *J. Biol. Chem. 277*, 9625–9628.
6. Falke, J. J., and Hazelbauer, G. L. (2001) Transmembrane signaling in bacterial chemoreceptors. *Trends Biochem. Sci. 26*, 257–265.
7. Studdert, C. A., and Parkinson, J. S. (2004) Crosslinking snapshots of bacterial chemoreceptor squads. *Proc. Natl. Acad. Sci. U.S.A. 101*, 2117–2122.
8. Kim, K. K., Yokota, H., and Kim, S. H. (1999) Four-helical-bundle structure of the cytoplasmic domain of a serine chemotaxis receptor. *Nature 400*, 787–792.
9. Khursigara, C. M., Wu, X., and Subramaniam, S. (2008) Chemoreceptors in *Caulobacter crescentus*: Trimers of receptor dimers in a partially ordered hexagonally packed array. *J. Bacteriol. 190*, 6805–6810.
10. Briegel, A., Ding, H. J., Li, Z., Werner, J., Gitai, Z., Dias, D. P., Jensen, R. B., and Jensen, G. J. (2008) Location and architecture of the *Caulobacter crescentus* chemoreceptor array. *Mol. Microbiol. 69*, 30–41.
11. Zhang, P., Khursigara, C. M., Hartnell, L. M., and Subramaniam, S. (2007) Direct visualization of *Escherichia coli* chemotaxis receptor arrays using cryo-electron microscopy. *Proc. Natl. Acad. Sci. U.S.A. 104*, 3777–3781.
12. Sourjik, V., and Berg, H. C. (2000) Localization of components of the chemotaxis machinery of *Escherichia coli* using fluorescent protein fusions. *Mol. Microbiol. 37*, 740–751.
13. Maddock, J. R., and Shapiro, L. (1993) Polar location of the chemoreceptor complex in the *Escherichia coli* cell. *Science 259*, 1717–1723.
14. Bray, D., Levin, M. D., and Morton-Firth, C. J. (1998) Receptor clustering as a cellular mechanism to control sensitivity [see comments]. *Nature 393*, 85–88.
15. Segall, J. E., Block, S. M., and Berg, H. C. (1986) Temporal comparisons in bacterial chemotaxis. *Proc. Natl. Acad. Sci. U.S.A. 83*, 8987–8991.
16. Erbse, A. H., and Falke, J. J. (2009) The Core Signaling Proteins of Bacterial Chemotaxis Assemble To Form an Ultrastable Complex. *Biochemistry. 48*, 6975–6987.
17. Falke, J. J., and Kim, S. H. (2000) Structure of a conserved receptor domain that regulates kinase activity: The cytoplasmic domain of bacterial taxis receptors. *Curr. Opin. Struct. Biol. 10*, 462–469.
18. Milburn, M. V., Prive, G. G., Milligan, D. L., Scott, W. G., Yeh, J., Jancarik, J., Koshland, D. E.Jr., and Kim, S. H. (1991) Three-dimensional structures of the ligand-binding domain of the bacterial aspartate receptor with and without a ligand. *Science 254*, 1342–1347.
19. Miller, A. S., and Falke, J. J. (2004) Side chains at the membrane-water interface modulate the signaling state of a transmembrane receptor. *Biochemistry 43*, 1763–1770.
20. Swain, K. E., and Falke, J. J. (2007) Structure of the Conserved HAMP Domain in an Intact, Membrane-Bound Chemoreceptor: A Disulfide Mapping Study. *Biochemistry 46*, 13684–13695.

21. Hulko, M., Berndt, F., Gruber, M., Linder, J. U., Truffault, V., Schultz, A., Martin, J., Schultz, J. E., Lupas, A. N., and Coles, M. (2006) The HAMP domain structure implies helix rotation in transmembrane signaling. *Cell 126*, 929–940.
22. Alexander, R. P., and Zhulin, I. B. (2007) Evolutionary genomics reveals conserved structural determinants of signaling and adaptation in microbial chemoreceptors. *Proc. Natl. Acad. Sci. U.S.A. 104*, 2885–2890.
23. Starrett, D. J., and Falke, J. J. (2005) Adaptation mechanism of the aspartate receptor: Electrostatics of the adaptation subdomain play a key role in modulating kinase activity. *Biochemistry 44*, 1550–1560.
24. Pollard, A. M., Bilwes, A. M., and Crane, B. R. (2009) The structure of a soluble chemoreceptor suggests a mechanism for propagating conformational signals. *Biochemistry 48*, 1936–1944.
25. Park, S. Y., Borbat, P. P., Gonzalez-Bonet, G., Bhatnagar, J., Pollard, A. M., Freed, J. H., Bilwes, A. M., and Crane, B. R. (2006) Reconstruction of the chemotaxis receptor-kinase assembly. *Nat. Struct. Mol. Biol. 13*, 400–407.
26. Coleman, M. D., Bass, R. B., Mehan, R. S., and Falke, J. J. (2005) Conserved glycine residues in the cytoplasmic domain of the aspartate receptor play essential roles in kinase coupling and on-off switching. *Biochemistry 44*, 7687–7695.
27. Bass, R. B., Miller, A. S., Gloor, S. L., and Falke, J. J. (2007) The PICM Chemical Scanning Method for Identifying Domain-Domain and Protein-Protein Interfaces: Applications to the Core Signaling Complex of *E. coli* Chemotaxis. *Methods Enzymol. 423*, 1–24.
28. Miller, A. S., Kohout, S. C., Gilman, K. A., and Falke, J. J. (2006) CheA Kinase of bacterial chemotaxis: chemical mapping of four essential docking sites. *Biochemistry 45*, 8699–8711.
29. Mehan, R. S., White, N. C., and Falke, J. J. (2003) Mapping out regions on the surface of the aspartate receptor that are essential for kinase activation. *Biochemistry 42*, 2952–2959.
30. Ames, P., and Parkinson, J. S. (1994) Constitutively signaling fragments of Tsr, the *Escherichia coli* serine chemoreceptor. *J. Bacteriol. 176*, 6340–6348.
31. Liu, J. D., and Parkinson, J. S. (1991) Genetic evidence for interaction between the CheW and Tsr proteins during chemoreceptor signaling by *Escherichia coli*. *J. Bacteriol. 173*, 4941–4951.
32. Bass, R. B., Butler, S. L., Chervitz, S. A., Gloor, S. L., and Falke, J. J. (2007) Use of site-directed cysteine and disulfide chemistry to probe protein structure and dynamics: Applications to soluble and transmembrane receptors of bacterial chemotaxis. *Methods Enzymol. 423*, 25–51.
33. Winston, S. E., Mehan, R., and Falke, J. J. (2005) Evidence that the adaptation region of the aspartate receptor is a dynamic four-helix bundle: Cysteine and disulfide scanning studies. *Biochemistry 44*, 12655–12666.
34. Bass, R. B., and Falke, J. J. (1999) The aspartate receptor cytoplasmic domain: In situ chemical analysis of structure, mechanism and dynamics. *Structure 7*, 829–840.
35. Bass, R. B., Coleman, M. D., and Falke, J. J. (1999) Signaling domain of the aspartate receptor is a helical hairpin with a localized kinase docking surface: Cysteine and disulfide scanning studies. *Biochemistry 38*, 9317–9327.
36. Danielson, M. A., Bass, R. B., and Falke, J. J. (1997) Cysteine and disulfide scanning reveals a regulatory α-helix in the cytoplasmic domain of the aspartate receptor. *J. Biol. Chem. 272*, 32878–32888.
37. Bass, R. B., and Falke, J. J. (1998) Detection of a conserved α-helix in the kinase-docking region of the aspartate receptor by cysteine and disulfide scanning. *J. Biol. Chem. 273*, 25006–25014.
38. Walshaw, J., and Woolfson, D. N. (2003) Extended knobs-into-holes packing in classical and complex coiled-coil assemblies. *J. Struct. Biol. 144*, 349–361.
39. Walshaw, J., and Woolfson, D. N. (2001) Socket: A program for identifying and analysing coiled-coil motifs within protein structures. *J. Mol. Biol. 307*, 1427–1450.
40. Chervitz, S. A., Lin, C. M., and Falke, J. J. (1995) Transmembrane signaling by the aspartate receptor: Engineered disulfides reveal static regions of the subunit interface. *Biochemistry 34*, 9722–9733.
41. Adler, J. (1969) Chemoreceptors in bacteria. *Science 166*, 1588–1597.
42. Chervitz, S. A., and Falke, J. J. (1995) Lock on/off disulfides identify the transmembrane signaling helix of the aspartate receptor. *J. Biol. Chem. 270*, 24043–24053.
43. Studdert, C. A., and Parkinson, J. S. (2005) Insights into the organization and dynamics of bacterial chemoreceptor clusters through in vivo crosslinking studies. *Proc. Natl. Acad. Sci. U.S.A. 102*, 15623–15628.
44. Bornhorst, J. A., and Falke, J. J. (2001) Evidence that both ligand binding and covalent adaptation drive a two-state equilibrium in the aspartate receptor signaling complex. *J. Gen. Physiol. 118*, 693–710.
45. Vaknin, A., and Berg, H. C. (2008) Direct evidence for coupling between bacterial chemoreceptors. *J. Mol. Biol. 382*, 573–577.
46. Lai, W. C., Beel, B. D., and Hazelbauer, G. L. (2006) Adaptational modification and ligand occupancy have opposite effects on positioning of the transmembrane signalling helix of a chemoreceptor. *Mol. Microbiol. 61*, 1081–1090.
47. Kim, S. H. (1994) "Frozen" dynamic dimer model for transmembrane signaling in bacterial chemotaxis receptors. *Protein Sci. 3*, 159–165.
48. Ames, P., Yu, Y. A., and Parkinson, J. S. (1996) Methylation segments are not required for chemotactic signalling by cytoplasmic fragments of Tsr, the methyl-accepting serine chemoreceptor of *Escherichia coli*. *Mol. Microbiol. 19*, 737–746.
49. Gloor, S. L., and Falke, J. J. (2009) Thermal domain motions of CheA kinase in solution: Disulfide trapping reveals the motional constraints leading to trans-autophosphorylation. *Biochemistry 48*, 3631–3644.
50. Hamel, D. J., Zhou, H., Starich, M. R., Byrd, R. A., and Dahlquist, F. W. (2006) Chemical-shift-perturbation mapping of the phosphotransfer and catalytic domain interaction in the histidine autokinase CheA from *Thermotoga maritima*. *Biochemistry 45*, 9509–9517.
51. Boldog, T., Grimme, S., Li, M., Sligar, S. G., and Hazelbauer, G. L. (2006) Nanodiscs separate chemoreceptor oligomeric states and reveal their signaling properties. *Proc. Natl. Acad. Sci. U.S.A. 103*, 11509–11514.